GEOPHYSICAL RESEARCH LETTERS, VOL. 23, NO. 2, PAGES 141-144, JANUARY 15, 1996

Mesopause temperature profiling by potassium lidar

Ulf von Zahn and Josef Höffner
Institut für Atmosphärenphysik, Kühlungsborn, Germany

Abstract. We report on initial measurements of potassium density and temperature profiles of the mesopause region by a containerized and hence transportable lidar instrument. The centerpiece of this lidar is a new, all-solid-state laser system. We employed a cw seeded and pulsed alexandrite ring laser working at the 770 nm wavelength of the $K(D_1)$ finestructure line. We show that, different from the Na case, in K soundings the effects of a minor isotope have to be taken into account in the data analysis. We point out that we observe on average considerably smaller K column densities than those published in the late 1970s by a French group. We study quantitatively the influence of the Hanle and potential saturation effects on the derived temperatures. We give an example of a mesopause temperature profile taken with our transportable K lidar.

Introduction

The thermal structure of the mesopause region, even though being of major interest to atmospheric scientists, is still only marginally explored. This is largely because of the general inaccessibility of this region. In the past decade, active remote sensing by groundbased lidar of the Doppler width of the $Na(D_2)$ resonance line at 589 nm wavelength has been developed into the foremost method to measure accurate temperature profiles in the 80 to 110 km altitude region [*Neuber et al.,* 1988; *She et al.,* 1992]. This technique has in addition led to the discovery of major and unpredicted temperature anomalies in the midlatitude mesopause region [*She et al.,* 1993]. But even before this discovery was made, it was recognized that it is highly desirable to make Doppler temperature lidars transportable. Their temperature soundings, performed at a variety of geographic locations and seasons, would reveal the complex thermal structure of the mesopause region. To this end we have developed and field-proven an all-solid-state laser which combines high-quality laser emissions with small overall volume and ease of operation. This laser forms the heart of a containerized and thus transportable Doppler temperatur lidar system. This temperature lidar is the first one to work on a potassium finestructure line (instead of sodium). In this way, the lidar does not only sample new temperature information, but also data on the little known mesospheric K densities, their altitude distributions and seasonal variations. Here we present technological and initial geophysical results obtained with this new lidar system.

Instrumentation

Our K lidar consists basically of (1) an alexandrite ring laser, which is injection seeded by a laser diode, (2) a wavelength meter, which is used to measure precisely the wavelengths of the emitted laser pulses, (3) a receiving telescope, and (4) a single photon counting device with computer, all installed in a 20 ft standard container. The container is currently located at our field station in Juliusruh on the German island Rügen (54°N, 13°E).

The unidirectional alexandrite ring laser is injection seeded by a laser diode. Its light is linearly polarised, its pulses have an average output energy of 100 mJ and a duration of 275 ns. The laser is operated with 25 pulses/s, and is tunable from pulse to pulse over a range > 50 pm [*Schmitz et al.,* 1995]. The large pulse length allows for an ultra-narrow spectral width of the pulses and helps to avoid saturation effects of K atoms in the potassium layer. The spectral width of the laser pulses is measured pulse-by-pulse with a high-resolution spectrum analyzer. About 99% of all laser pulses are in a TEM_{00} mode and have a spectral width lower than the resolution of our spectrum analyser (20 MHz). The exact wavelength of each laser pulse is measured pulse-by-pulse with a wavemeter, the heart of which is a Fabry-Perot interferometer with 5.2 cm plate spacing. Its interference fringes are imaged onto a linear array of 1024 photodiodes. The data from these diodes are used to calculate in realtime the relative wavelength of each pulse and to control the spectral purity.

The receiving telescope uses a mirror with 80 cm diameter. At its focus a fiber cable picks up the photons for transport to the optical bench. The single-photon counting system has an altitude resolution of 200 m. Depending on the measured wavelength of the laser pulse, individual counts are collected in one of 18 data channels, each being 0.16 pm wide.

Atomic Data and Temperature Analysis

The most abundant potassium isotope is ^{39}K with an isotopic abundance of 93.1%. The $K(D_1)$ finestructure line has an air wavelength of 769.898 nm (the $K(D_2)$ line at 766.491 nm can not be used for groundbased lidar soundings as it is imbedded in a strong O_2 absorption line). The $K(D_1)$ line consists of 4 hyperfine structure lines, the quantum numbers, frequency offsets, and relative line strengths are given in Table 1.

The maximum of the $^{39}K(D_1)$ backscatter cross section is $d\sigma_{max}(180°)/d\Omega = 7.65 \times 10^{-17}$ [m^2/ster] for 200 K. It is nearly equal to that of the $Na(D_{2a})$ component. In comparison to Na, the K hfs transitions are, however, closer together and this results in

Table 1. Quantum numbers, frequency offsets and relative line strength for the $K(D_1)$ hfs lines calculated from Saloman [1993].

$S_{1/2}$	$P_{1/2}$	^{39}K [MHz]	^{41}K [MHz]	relative line strength
F=1	F=2	310	405	5
	F=1	254	375	1
F=2	F=2	-152	151	5
	F=1	-208	121	5

Paper number 95GL03688
0094-8534/96/95GL-03688$03.00

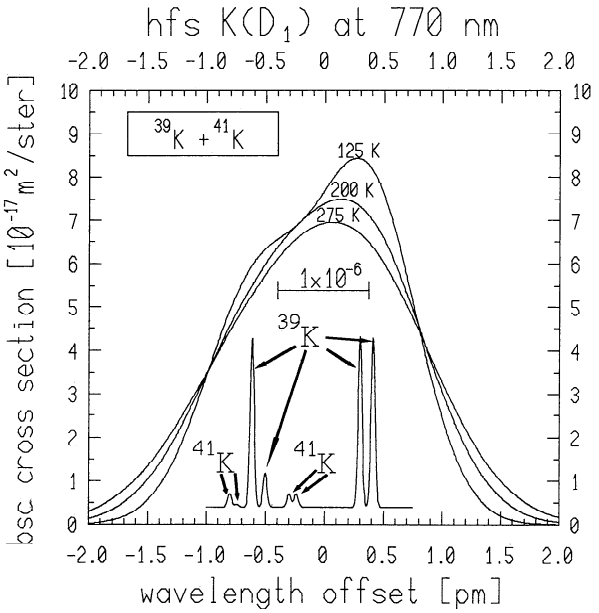

Figure 1: Variation of the backscatter cross section of the $K(D_1)$ transition with temperature for $^{39}K+^{41}K$. The positions and relative strengths of the hyperfine transitions are indicated. The FWHM of these transitions is plotted with the estimated maximum bandwidth of the used laser (20 MHz).

a more nearly Gaussian shape for the $K(D_1)$ backscatter cross section for temperatures above, say, 175 K. At lower temperatures, the $K(D_1)$ line shape becomes noticeably non-Gaussian.

The presence of the minor isotope ^{41}K with an abundance of 6.9% changes moderately the shape of the $K(D_1)$ fine structure line and has to be taken into account during data analysis. With respect to the ^{39}K line, the center of the ^{41}K line is shifted towards shorter wavelengths and the hfs transitions are somewhat closer together (see Table 1). Figure 1 shows the resulting shape of the D_1 fine structure line together with the hfs transitions and their relative line strengths. Inclusion of the ^{41}K isotope decreases the maximum backscatter cross section to $7.51x10^{-17}$ [m^2/ster].

For a natural mixture of ^{39}K and ^{41}K, the variation of the FWHM of the $K(D_1)$ line vs. temperature is shown in Figure 2. At 200 K, the linewidth is 1.85 pm. To determine the FWHM of the received signal, the resonance backscatter cross section, convoluted with the laser bandwidth and assumed gaussian line

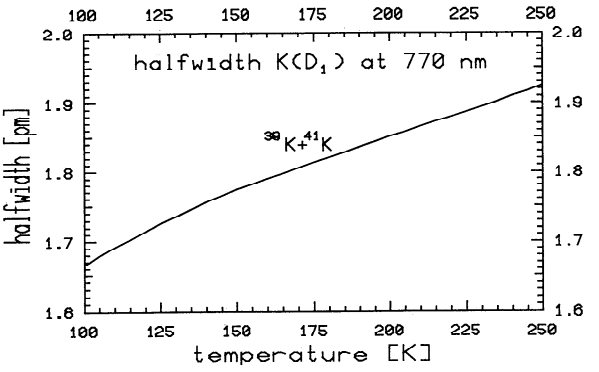

Figure 2: Variation of the FWHM of the backscatter cross section of $K(D_1)$ with temperature for $^{39}K+^{41}K$. The gradient is about 0.0017 pm/K.

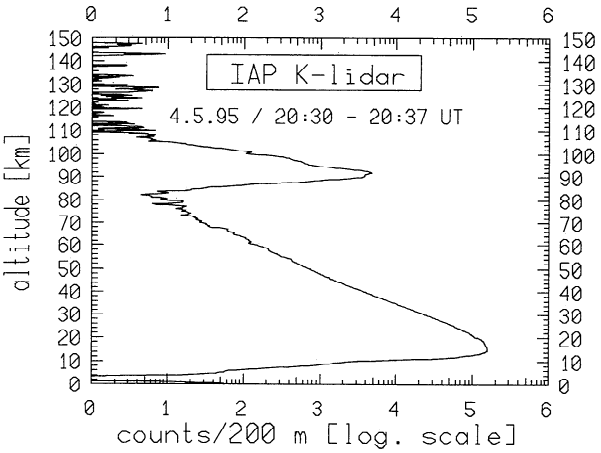

Figure 3: Count rate profile with 200 m altitude resolution (smoothed 1:2:4:2:1), background substracted, measured May 4, 1995. Integration time 7 min (= 10000 laser pulses).

shape, is least-squares-fitted to the lidar-observed line shape. The temperature is then derived from the parameters of the fit.

Potassium Densities

Figure 3 shows a count rate profile of our K-lidar as observed on May 4, 1995 between 20:30 UT and 20:37 UT. A background of 16 counts/200 m is already subtracted. The signal from the potassium layer between 80 km and 105 km altitude reaches about 5000 counts/200 m. The Rayleigh signal disappears in the atom resonance signal from the potassium layer near 82 km. This condition will make it possible to calculate Rayleigh temperatures with an upper boundary temperature taken from the potassium measurement. Below 20 km the Rayleigh signal is blocked by a mechanical light chopper to protect the detector.

Figure 4 shows the observed mean K number density profiles for February and May 1995. In February the maximum density at 88 km altitude was 30 atoms/cm^3 with a column density of $4x10^7$ atoms/cm^2. The layer was rather broad and reached from below

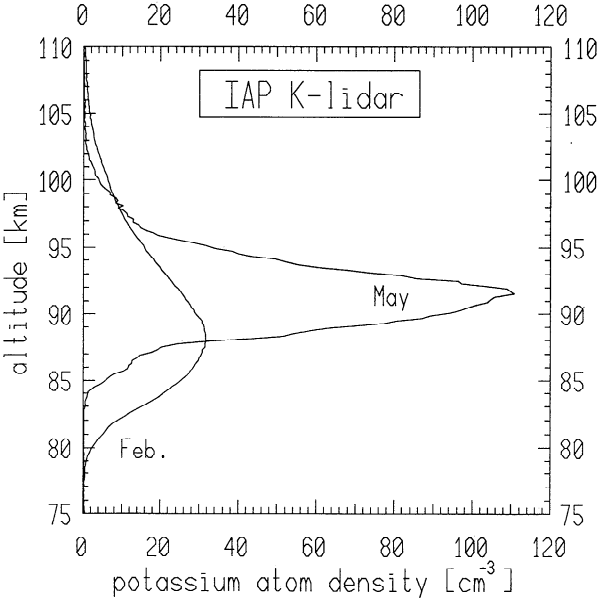

Figure 4: Monthly mean K number density profiles for February and May, 1995.

Table 2. Potassium column density and peak density, observed in twilight and by lidar.

authors	column density [10^7 cm^{-2}]	peak density [cm^{-3}]
Sullivan and Hunten [1964]	5.6	25
Gault and Rundle [1968]	8	-
Felix et al. [1973]	9	-
Mégie et al. [1978]	30	300
Nagasawa and Abo [1994]	-	60-100
this work	4-7	30-120

80 km to above 105 km altitude. In May the situation is considerably different. The layer is now much smaller and at a higher altitude. The layer peak is near 91 km altitude with about 100 atoms/cm^3. The column density is 6.6x10^7 atoms/cm^2. Quite noticeable is the change in the shape and altitude of the layer from February to May. If this change is indeed a seasonal variation, then it is about opposite to how the sodium layer behaves [*Kurzawa and von Zahn,* 1990].

As Table 2 shows, our observed K densities agree quite well with the results of earlier twilight observations and the lidar measurements of Nagasawa and Abo [1994]. It is not understood why the lidar observations of Megie et al. [1978] indicate noticeably higher K densities and very little seasonsal variation of these.

Temperature Profiles

Temperatures are derived from the accurately measured shape of the K(D$_1$) finestructure line. As an example of measured line shapes, Figure 5 shows data (open circles) obtained during the night of May 4./5., 1995 for different altitudes and an integration period of about 3 hours. The least squares fits are calculated over altitude ranges of 2 km, but with 1 km separation from each other.

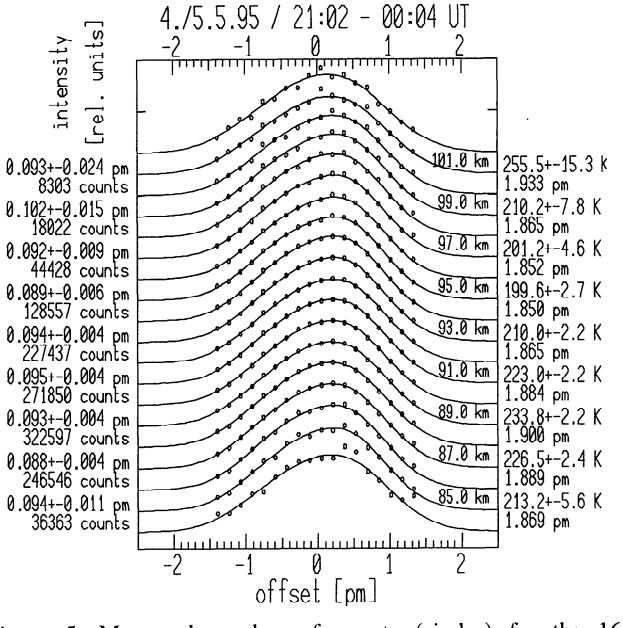

Figure 5: Measured number of counts (circles) for the 16 wavelength channels and computer fits (solid lines) for the K(D$_1$) finestructure line at different altitudes. Information on the numbers on either side of the curves is given in the text.

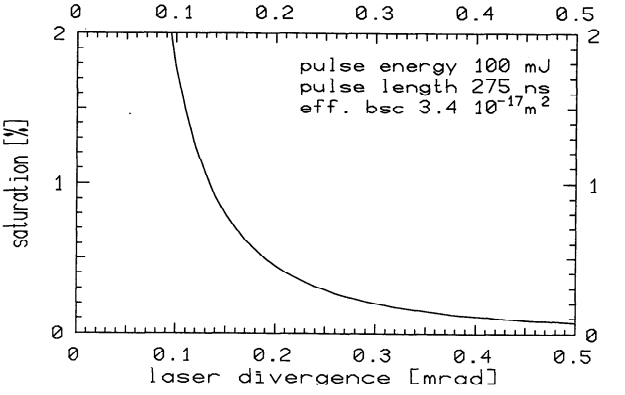

Figure 6: Dependence of the degree of saturation (in %) on the laser beam divergence for one of the strong hfs lines of ^{39}K, calculated for a laser pulse of 100 mJ energy and 275 ns duration, and K layer height of 90 km.

Important parameters of the fits are listed on both sides of each profile. On the left side, the upper values are the offsets of the line maxima from an arbitrary wavelength "zero". Below are the total photon counts over the entire line. On the right side, the upper value gives the calculated temperature and its error. Errors are one sigma errors of the least-squares-fit excluding systematic errors. The largest potential source for systematic errors is the accuracy of our wavemeter calibration (estimated contribution about ± 5 K). Because of our ultra-narrow laser bandwidth, systematic errors stemming from the convolution of laser bandwidth with the backscatter cross section should be very small, that is < 0.5 K. We point out, that for linearly polarised laser light, the Hanle effect of the K(D$_1$)-resonance process equals one [*Zimmermann,* 1975]. It means that the backscattered intensity is independent of the geomagnetic field.

In our experiment, corrections of the calculated temperature value due to saturation effects in the K layer are negligible. This

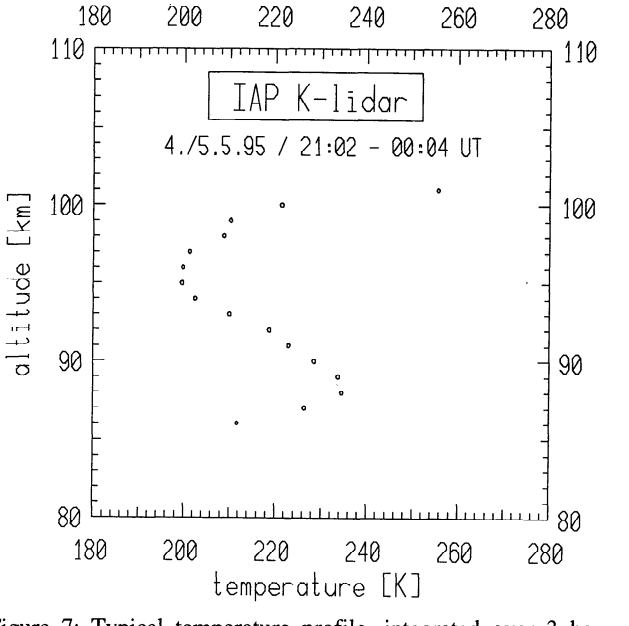

Figure 7: Typical temperature profile, integrated over 3 hours during May 4, 1995 for ^{39}K+^{41}K. The statistical 1σ-error at the maximum of the potassium layer is ± 2 K. For a discussion of systematic errors, see text.

is demonstrated in Figure 6 showing the degree of saturation (in percent) depending on the divergence of a 100 mJ laser beam.

For the parameters of our laser (divergence of 0.4 mrad and pulse length of 275 ns) the saturation is less than 0.2% for one of the hfs lines. Computer simulations for determining the temperature shows that even a saturation of 10% would change the temperature only about 0.2 K. The reason for such a small influence of saturation effects on the calculated temperature is the fact that the three strongest hfs lines all have the same line strength and therefore always exhibit the same degree of saturation. Only one hfs transition has a much smaller line strength, but due to its spectral position between the strong lines and because of its small line strength, it has only a marginal influence on the overall line shape and hence temperature determination.

Figure 7 shows an example of a measured temperature profile, calculated taking both K isotopes into account. The data were aquired late at night of May 4, 1995 and integrated over 3 hours. The mesopause has a temperature of 200 K at an altitude of 96 km. The local maximum in the temperature near 89 km is due to strong wave activity during the whole night which we can recognize when integrating over shorter time periods. The uncomfortably long integration time is basically due to the unexpectedly low K densities, the latter reaching only a few percent of the Na densities. The negative effects of these small K densities for our K lidar are to some extent compensated by the much higher pulse energy of our alexandrite laser over the (narrowband) dye lasers used for Na lidars. Another fact contributing to our low count rates is that our current laser system is not optimized yet for operations at 770 nm wavelength. The laser has still an ample potential for further improvements.

Conclusion

We have demonstrated the feasibility to perform remote sensing measurements of temperature profiles in the mesopause region by a potassium lidar. In comparison to Na lidars, K lidars offer negligible saturation effects and a Hanle effect which is 1 for linearly polarised laser beams. For this experiment we have developed an ultra-narrowband, high power, all-solid-state laser which is still small and light enough to be transportable in a containerized lidar system. The complete instrument fits inside a standard 20 ft container. An initial series of measurements of K density profiles at 54°N latitude shows considerably lower densities than published by Megie et al. (1978) and peak K densities in May being much higher than in February. If interpreted as a seasonal change, this behaviour would be opposite to the behaviour of sodium in the upper mesosphere.

Acknowledgments. We acknowledge with pleasure the great contributions of St. Schmitz during the development of our current laser system. M. Alpers and V. Eska have been a great help in getting the lidar system to work at Juliusruh and in data collection. We appreciated fruitful discussions with C.Y. She. The early part of this project was funded by the Deutsche Forschungsgemeinschaft under grant no. Za 83/5.

References

Felix, F., W. Keenliside, G. Kent, and M.C.W. Sandford, Laser radar observations of atmospheric potassium, *Nature, 246,* 1972-1973, 1973.

Gault, W.A., and H.N. Rundle, Twilight observations of upper atmospheric sodium, potassium, and lithium, *Can. J. Phys., 47,* 85-98, 1969.

Kurzawa, H., and U. von Zahn, Sodium density and atmospheric temperature in the mesopause region in polar summer, *J. Atmos. Terr. Phys., 52,* 981-993, 1990.

Mégie, G., F. Bos, J.E. Blamont, and M.L. Chanin, Simultaneous nighttime lidar measurements of atmospheric sodium and potassium, *Planet. Space Sci., 26,* 27 - 35, 1978.

Nagasawa, C., and M. Abo, Lidar measurements on mesospheric metallic atom layers, paper presented at 96th Meeting Soc. Geomagn. and Earth, Planetary and Space Sciences, Nagoya, Japan, 1994.

Neuber, R., P. von der Gathen, and U. von Zahn, Altitude and temperature of the mesopause at 69°N latitude in winter, *J. Geophys. Res., 93,* 11093-11101, 1988.

Saloman, E.B., A resonance ionization spectroscopy/resonance ionization mass spectrometry data service. IV-Data sheets for Be, In, Li, K, Rb, Ag, Ti, and V and an update of the data sheet for Ni, *Spectrochimica Acta, 48B,* 1139-1203, 1993.

Schmitz, S., U. von Zahn, J.C. Walling, and D. Heller, Alexandrite lasers for temperature sounding of the sodium layer, in *Proc. 12th ESA Symp. on European Rocket and Ballon Programmes and Related Research,* Lillehammer, Norway, 29 May - 1 June, 1995.

She, C.Y., J.R. Yu, H. Latifi, and R.E. Bills, High-spectral-resolution fluorescence light detection and ranging for mesospheric sodium temperature measurements, *Appl. Optics, 31,* 2095-2106, 1992.

She, C.Y., J.R. Yu, and H. Chen, Observed thermal structure of a midlatitude mesopause, *Geophys. Res. Lett., 20,* 567-570, 1993.

Sullivan, H.M., and D.M. Hunten, Lithium, sodium, and potassium in the twilight airglow, *Can. J. Phys., 42,* 937-956, 1964.

Zimmermann, D., Determination of the lifetime of the $4P_{1/2}$-state of potassium by Hanle-effect, *Z. Phys., A275,* 5-10, 1975.

J. Höffner and U. von Zahn, Institut für Atmosphärenphysik an der Universität Rostock e.V., Schloßstr. 4-6, D-18221 Ostseebad Kühlungsborn, Germany. (e-mail: hoeffner@iap-kborn.d400.de; uvonzahn@apollo1.iap-kborn.de)

Received: October 23, 1995; accepted: November 24, 1995